

Lawrence Berkeley National Laboratory

Lawrence Berkeley National Laboratory

Title

Towards sub-10 nm resolution zone plates using the overlay nanofabrication processes

Permalink

<https://escholarship.org/uc/item/39x5008f>

Authors

Chao, Weilun
Anderson, Erik H.
Fischer, Peter
et al.

Publication Date

2008-05-23

Towards sub-10 nm resolution zone plates using the overlay nanofabrication processes

Weilun Chao^{1*}, Erik H. Anderson¹, Peter Fischer¹, and Dong-Hyun Kim²

¹Center for X-ray Optics, Lawrence Berkeley National Laboratory, 1 Cyclotron Road, MS 2-400, Berkeley, CA 94720

²Department of Physics, Chungbuk National University, Cheongju 361-763, Chungbuk, South Korea

ABSTRACT

Soft x-ray zone plate microscopy has proven to be a valuable imaging technique for nanoscale studies. It complements nano-analytic techniques such as electron and scanning probe microscopies. One of its key features is high spatial resolution. We developed an overlay nanofabrication process which allows zone plates of sub-20 nm zone widths to be fabricated. Zone plates of 15 nm outer zones were successfully realized using this process, and sub-15 nm resolution was achieved with these zone plates. We extend the overlay process to fabricating zone plates of 12 nm outer zones, which is expected to achieve 10 nm resolution. In addition, we have identified a pathway to realizing sub-10 nm resolution, high efficiency zone plates with tilted zones using the overlay process.

Keywords: zone plates, spatial resolution, x-ray microscopy, electron beam lithography, overlay fabrication technique

1. INTRODUCTION

Since the pioneering work by Schmahl's group^{1,2} and Kirz's group³, soft x-ray zone plate microscopy⁴⁻¹¹ has become a valuable tool to many nanoscience and nanotechnology studies. The technique takes advantage of the short wavelengths and the existence of low-Z elements' transition edges in the soft x-ray region¹². It provides a unique set of capabilities including high spatial resolution, natural elemental/chemical and magnetic sensitivities, large permissible sample thickness, and a myriad of in-situ sample environments. The capabilities complements nano-analytic techniques such as electron and scanning probe microscopies. A wide range of sciences and technologies, including inter- and sub-cellular biology, nanomagnetism, wet environmental studies, and semiconductor technology, have gained valuable information using the microscopy⁴⁻¹¹. The goal of this work is to improve the spatial resolution of soft x-ray microscopy to 10 nm and beyond.

2. CHALLENGES TO HIGHER RESOLUTION AND OVERLAY FABRICATION TECHNIQUE

Soft x-rays generally refer to photons with energies from a few hundred eV to a few keV, or with wavelengths from less than 1 nm to about 4 nm. In this photon energy range, conventional optical lenses provide only limited performances due to strong material absorption and weak refraction¹². Fresnel zone plates, a circular diffractive optic, on the other hand, can provide high resolution with acceptable efficiency¹³, and have been commonly used in x-ray microscopy. The ideal spatial resolution¹⁴ of a zone plate is equal to $k_1\lambda/mNA$, where λ is the wavelength, NA is the numerical aperture of the imaging optic, k_1 is an illumination-dependent factor, and m is the diffraction order. For large magnification, $NA = \lambda/2\Delta r$, and the resolution can be expressed as $2k_1\Delta r/m$. Δr is the smallest (outermost) zone width of the optic. Two primary paths to higher resolution are (1) to reduce the outermost zone width and (2) to operate the zone plate lens in higher diffraction orders. As the diffraction efficiency for conventional zone plates decreases in higher diffraction

* wlchao@lbl.gov

orders¹², reducing the outermost zone width is the common pathway and has been actively pursued by various means worldwide.

High resolution zone plates, with narrow outer zones and accurate zone placement, are fabricated using electron beam lithography. The conventional fabrication process was published elsewhere¹⁵, and is briefly described here. The process starts with a substrate which is consisted of 100 nm thick low-stress silicon nitride membrane windows coated with a metal plating base, a layer of polymer, and a thin layer of high resolution e-beam resist. A zone plate pattern is exposed to the resist, which is subsequently developed, and the pattern is transferred to the polymer layer using plasma etching. Using the resist/polymer structure as a mold, electroplating is performed to form the desired zone plate structure, either with gold or nickel. The resist mold is then stripped away to complete the fabrication process. This commonly used process has been successfully yielded high quality zone plates with smallest zone widths down to 25 nm, achieving a resolution of 20 nm¹⁴. Smaller zone widths, however, are extremely difficult to achieve. Electron scattering, low resist resolution, finite beam size, and process development issues limits the smallest achievable period. For sub-20 nm zones, the regions where the resist should be removed after development for the subsequent plating have resist residue remained. Solution to this problem is not trivial and requires extensive resources and development.

Semi-dense lines, on the other hand, are less sensitive to these issues. Using various techniques such as over-development and ashing, one can achieve linewidths of 10 – 15 nm relatively easily and reliably. We based on this fact and developed a zone plate fabrication process, in which a zone plate pattern is divided into two (or more) semi-dense, complementary patterns (Fig. 1). The patterns are fabricated sequentially on the same substrate and are overlaid in high accuracy to form the desired zone plate pattern. The overlay technique can allow one to achieve pattern densities several times higher than would otherwise be possible. This concept is similar to the double exposure technique¹⁶, quite commonly utilized in semiconductor industry. However, to our knowledge, this is the first attempt to apply such concept to zone plate fabrication.

The key of success to this technique is the overlay accuracy. For zone plates, overlay accuracy better than one third of the smallest zone width is required to achieve diffraction limited resolution. To achieve such accuracy, an internally developed, sub-pixel resolution alignment algorithm, based on auto/cross-correlation methods¹⁷, is employed. The algorithm, which reliably provides sub-2nm accuracy, is performed in both complementary exposures, using the alignment mark sets that have been fabricated on the wafer substrates.

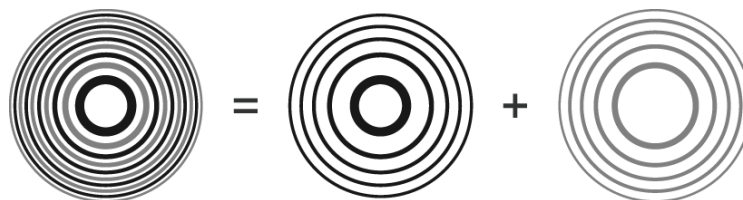


Figure 1 The concept of the zone plate overlay fabrication process. A dense zonal pattern is broken down to two semi-isolated, complementary patterns. Zone set I (black), and its complement, set II (grey), are fabricated sequentially on the same substrate and overlaid to form the desired zone plate pattern.

Fig. 2 illustrates the basic components of the zone plate overlay fabrication process. The fabrication process is composed of three sequential lithographic steps – alignment mark fabrication, first zone set fabrication, and second zone set fabrication. In the first step, four variants of the two-dimensional Barker alignment mark series, each of which is a rotated copy of the other, and a similar set of marks closer to the center, are fabricated on the substrate. Because the marks will be used for overlaying the subsequently fabricated zone patterns, as well as for the fine-calibration of the electron beam deflection, placement of the marks is critical. For this, the electron beam, and the major and minor field deflection of the electron beam system are carefully calibrated before the alignment mark exposure. The alignment marks are formed by electroplating in gold, and resist is removed from the substrate. After fabrication of the alignment marks, a fresh layer of resist is spin coated onto the substrate, and zone set I (black), with alternate zones missing, is

exposed at the center of the alignment marks. For best placement accuracy the electron beam position, and the beam deflector's scaling and orthogonality, are fine calibrated before each zone pattern exposure, using our alignment algorithm. Zone set I is then formed by electroplating in gold, and the resist is stripped from the substrate. In the third step, zone set II is fabricated, using the same process used for zone set I. By use of the alignment procedure before exposure, zone set II is exposed at the proper position with respect to the alignment marks, and thus also to zone set I, with similar accuracy. The outer alignment marks are used for alignment and fine calibration. The inner mark patterns are filled with gold during electroplating of zone set I, and thus are not available for set II. Zone set II is then formed by gold plating, in the same manner as for the zone set I. The individual steps of the fabrication process are shown in Fig. 3.

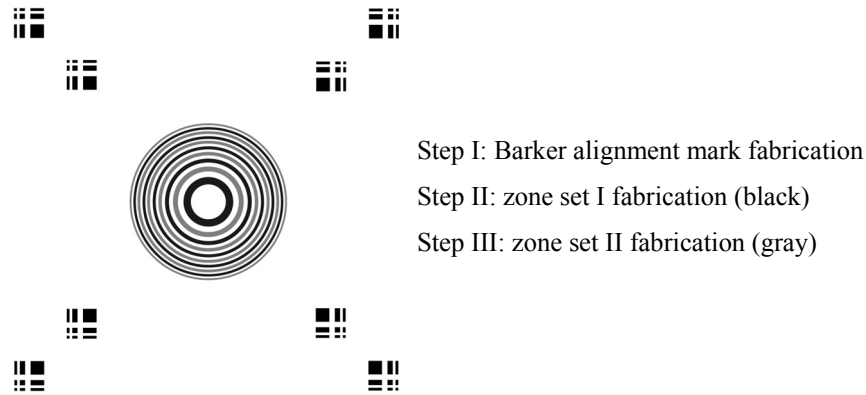


Figure 2 Illustration of the fabrication process for 15 nm micro zone plates. The complete process consists of three sequential lithographic steps: fabrication of Barker alignment marks, zone set I (black) fabrication, and zone set II (gray) fabrication. Fabrication of the two zone sets used the alignment marks for placement reference.

3. RESULTS

We have successfully fabricated, for the first time, zone plates of 15 nm outermost zones, using the overlay process as described in the last section. Fig. 4 shows the SEM micrograph of one of the zone plates. Written with a 2nm pixel, the 15 nm zone plate, of 500 zones and 30 μm in diameter, has an alignment accuracy of 1.7 nm, which well satisfies the zone placement requirement of 5 nm in this case. The complete zone plate fabrication was conducted in-house, using our 100 keV vector scan electron beam lithography system, the Nanowriter. The electron beam system, controlled by an internally designed digital pattern generator and electronics, were designed with particular attention to curved structure writing¹⁸. PMMA resist of 90 nm thick, and room temperature development with MIBK/IPA mixture were used in both zone set exposures. The gold zone structure was electroplated to 80 nm thick, giving an aspect ratio 5:1.

The zone plate was tested at the full-field transmission x-ray microscope^{19,20}, XM-1, at LBNL's Advanced Light Source (ALS). The XM-1 schematic is shown in the Fig. 5. To quantify the resolution achieved by this optic unambiguously, we employed multilayer coatings as test objects¹⁴. The multilayers, fabricated by magnetron sputtering, have nanometer precision control of layer thickness, making them ideal for resolution measurement. We processed the multilayers using the TEM sample thinning technique, and exposed the cross sections of the multilayers. We imaged the cross sections using the 15 nm zone plate. Fig. 6(a) shows an x-ray image of a 15.1 nm half-period Cr/Si multilayer test object, taken with a 15 nm zone plate, at the wavelength of 1.52 nm (815 eV photon energy). In comparison, an image of the same test object, taken with a 25 nm zone plate, which yielded the highest resolution of 20 nm achieved before this work, is shown in Fig. 6(b). A drastic improvement in resolution is achieved with the 15 nm zone plate. The image obtained by the new lens exhibits excellent modulation, whereas the image taken with our previous zone plate showed no modulation for the test pattern. Analysis of the image in Fig. 4(a), as well as other images of different multilayer periods, indicates that a resolution better than 15 nm has been achieved with the zone plate.

The zone plate has been used in nanomagnetic studies. Fig. 7 shows a soft x-ray image of a CrCoPt granular film recorded with the 15 nm zone plate, at the Co L_3 edge (777 eV photon energy, $\lambda = 1.60$ nm). With the sub-15 nm resolution, scientists quantify local magnetization hysteresis of the granular structures in nanoscale²¹. The knowledge acquired is useful to understanding of the fundamental behavior of nanomagnetism, and the development of future magnetic technology.

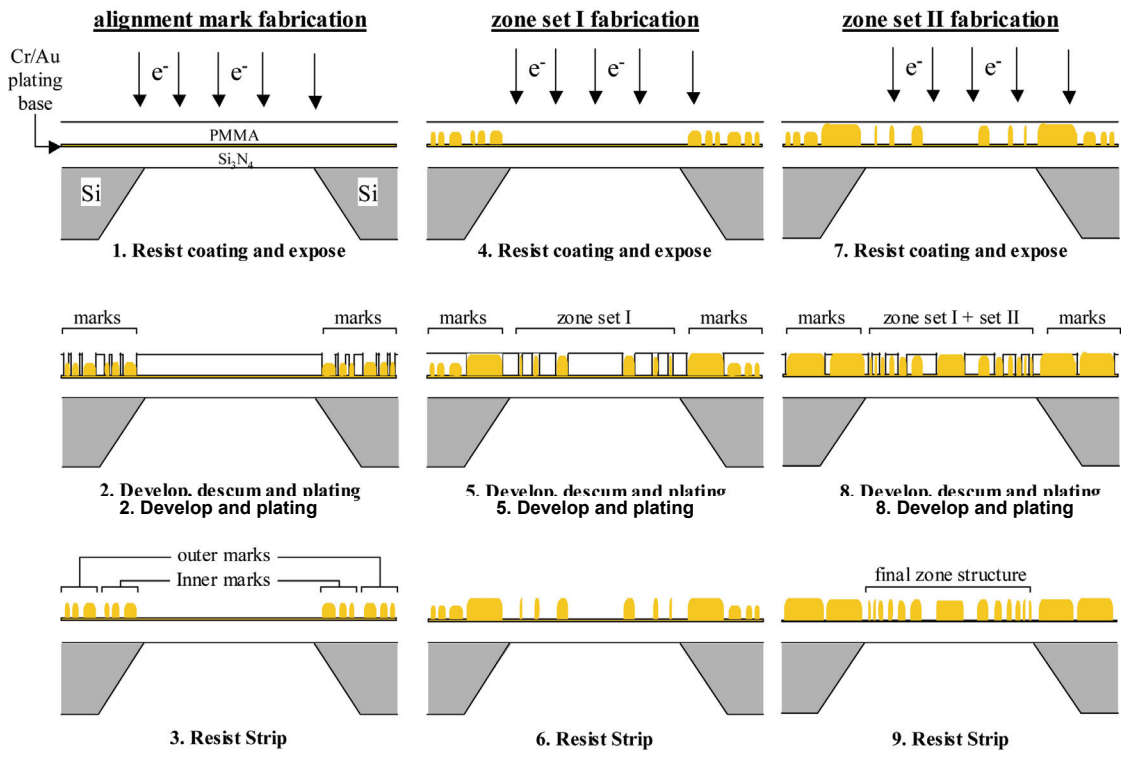


Figure 3 The details of the overlay nanofabrication process. The process has three sequential lithographic steps: alignment mark fabrication (left column), first zone set fabrication (middle column), and second zone set fabrication (right column). This process was used to fabricate the 15 nm zone plates. The 100 keV vector scan electron beam lithography system, the Nanowriter, at Lawrence Berkeley National Lab, was used to implement this process.

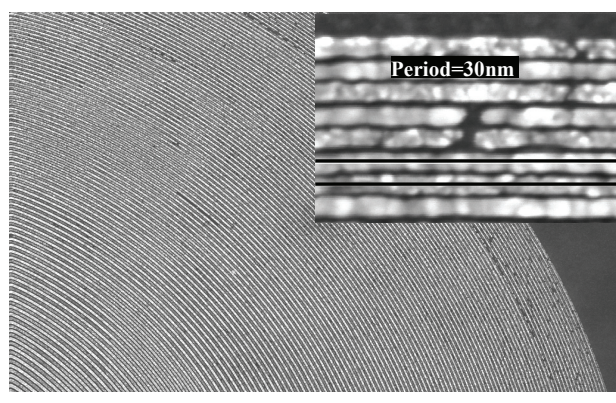


Figure 4 A scanning electron micrograph of a zone plate with 15 nm outermost zone width. Shown in the inset is a magnified view of the outer zone region. The zone placement accuracy is measured to be 1.7 nm.

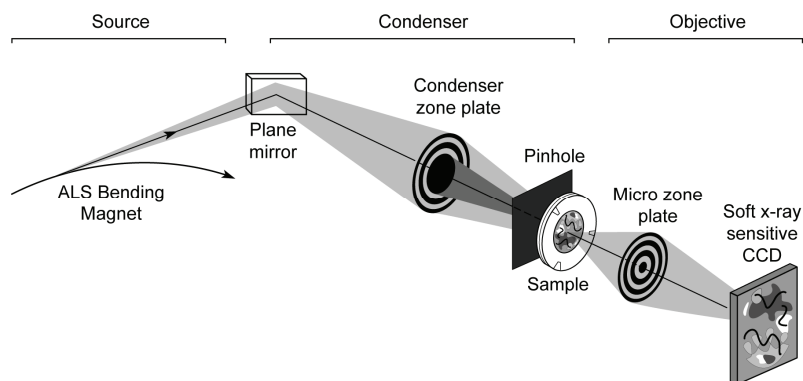


Figure 5 A schematic of the soft x-ray full-field microscope, XM-1, at the Advanced Light Source in Berkeley. The microscope uses a micro Fresnel zone plate to project a full field image onto a soft x-ray sensitive CCD camera. Hollow-cone illumination of the sample is provided by a condenser zone plate. The 15 nm zone plate was used as a micro zone plate in the experiment.

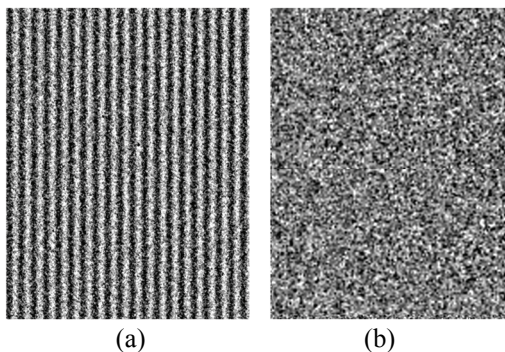


Figure 6 Soft x-ray images of a 15.1 nm half-period test object, obtained with zone plates having outer zone widths of 15 nm and 25 nm. The test object is a cross-section of Cr/Si multilayer with 15.1 nm half-period. Significant improvement is seen between the images obtained with the new 15 nm zone plate and with the 25 nm zone plate. (a) An image of 15.1 nm half-period with the 15 nm zone plate. (b) An image of 15.1 nm half-period with the previous 25 nm zone plate. Images (a) and (b) were obtained at a wavelength of 1.52 nm (815 eV photon energy) and 2.07 nm (600 eV), respectively.

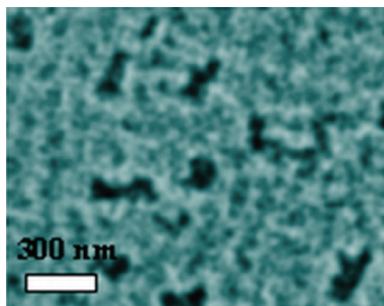


Figure 7 An soft x-ray image of a 50 nm thick nanogranular $(\text{Co}_{84}\text{Cr}_{16})_{87}\text{Pt}_{13}$ alloy film taken with a 15 nm zone plate. The high resolution of the zone plate enables scientists to study local magnetization hysteresis of this film in a nanoscale. The image was recorded at the Co L_3 edge (777 eV photon energy, $\lambda = 1.60$ nm).

We are currently applying the overlay process to fabricate even higher resolution zone plate. Fig. 8 shows an SEM micrograph of the first zone set of a 12 nm zone plate. The gold zone structure was obtained by developing the exposed PMMA at -20°C in 3:1 IPA:water. The second set, which is missing in the micrograph, is currently fabricated. With this zone plate, we expect a resolution of 10 nm at the XM-1 microscope.

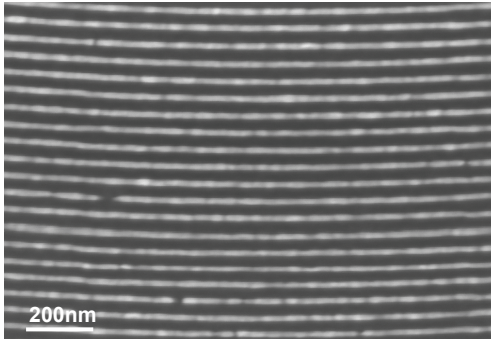


Figure 8 A scanning electron micrograph of the first zone set of two overlay patterns for a 12 nm outermost zone width zone plate. The second zone set is currently fabricated. Resolution of 10 nm is expected with this zone plate.

4. HIGHER RESOLUTION IN HIGHER DIFFRACTION ORDERS

While zone width reduction can yield higher resolution, operating zone plates at higher diffraction orders, as implied by the resolution formula in section 2, can drastically improve the resolution. The primary challenge of utilizing this fact is the extremely low efficiency at high diffraction orders. However, using electrodynamic theory calculation, G. Schneider²² showed that the efficiency at higher orders can be improved significantly, if the zones are tilted to satisfy the Bragg's condition at this diffraction order. Efficiency of more than 20% can be achieved at the 3rd order. For the common zone plate materials, gold or nickel, aspect ratios larger than 20 is required to achieve the improved efficiency.

To realize the tilt zone plates, Schneider²³ proposed to fabricate multilevel zone plates, where zone plates of slightly decreasing zone radii are stacked above the others (Fig. 9 (II)). The individual zone plates would have moderate aspect ratio. With accurate alignment of the zone plates, the composite structure would approximate a tilt zone plate. The key of success to this scheme is the accurate alignment of the individual zone plates. Depending on the diffraction order and number of layers, alignment accuracy of a few nanometers is required for achieving the improved efficiency. With our sub-pixel overlay accuracy, we identify a pathway to realizing the tilt zone plates with the requisite alignment accuracy using the overlay technique. Fig. 9 outlines the concept of the fabrication process.

As in the overlay fabrication used for the 15 nm zone plates, alignment marks are first fabricated onto the substrate (Fig. 9 steps 1a-1c). In the second step, the first level of the tilt zone plate, which is a conventional zone plate, is fabricated. The structure is accurately positioned relative to the inner alignment marks, by performing our alignment algorithm before the exposure (step 2b). The structure is formed by electroplating, and the resist mold is cross-linked to increase its robustness and insolubility for subsequent steps (step 2c). In the third step, a fresh layer of resist is spin coated onto the existing structure, and the same process as in the second step is used to form the second zone plate layer. A zone plate pattern, with slightly reduced zone radii, is exposed, with alignment to the outer set of alignment marks (step 3b). The pattern is then electroplated. To achieve multilevel structures, the same process steps are repeated, with each level aligned to the alignment marks, which in turn aligned to the other levels. This process involves a large number of steps, and challenges are anticipated. However, the overlay technique presented here addresses the alignment accuracy requirement, and can provide a viable means to realize the multilevel zone plates.

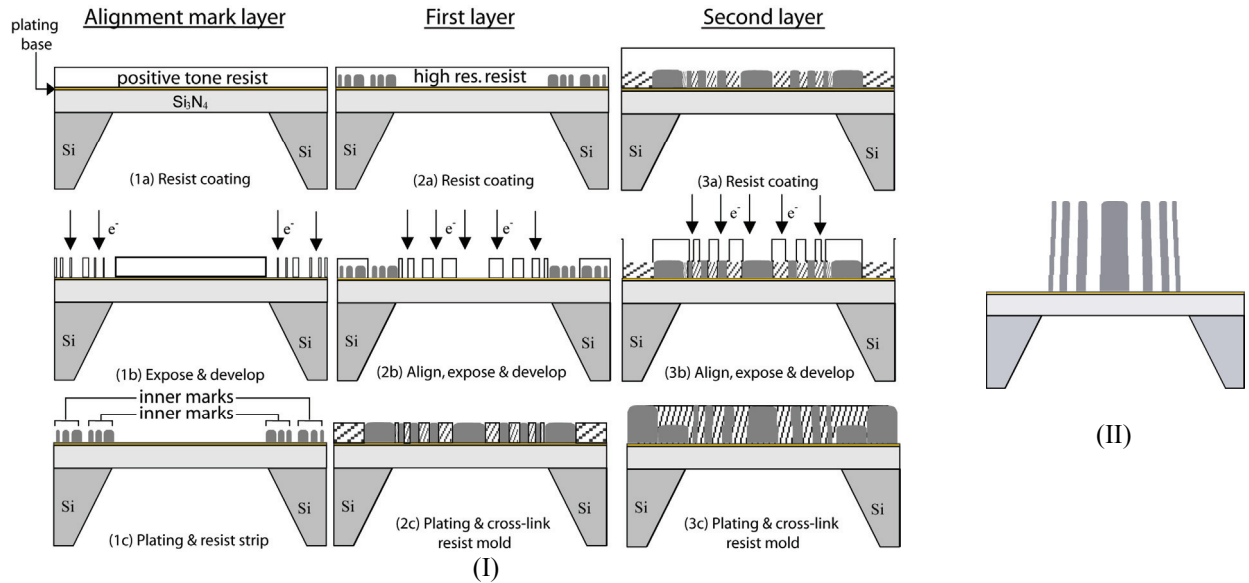


Figure 9 (I) Illustration of the fabrication process of multilevel zone plates using the overlay technique. The process starts with the fabrication of alignment marks on the substrate (step 1a-1c). Aligned to one set of the alignment marks, the first layer of the multilevel zone plate is then fabricated (step 2a-2c). A fresh resist is then spin coated above the zonal structure and the resist mold (step 3a). Aligned to the alignment marks, a zone plate pattern of slightly reduced zone radii is exposed, and fabricated into metal (step 3b and 3c). Steps 3a to 3c are then repeated for the other layers. After the last layer is fabricated, the resist mold from all previous steps is stripped off the substrate (not shown here). The illustration here depicts fabrication of only two levels. (II) A drawing of a five-level zone plate after the completion of fabrication. Alignment marks outside the zone plate are not shown here.

5. CONCLUSIONS

We have successfully developed a zone plate fabrication process based on overlay of two semi-isolated, complementary zone patterns. Zone plates of 15 nm outer zone width, which are not possible with conventional electron beam lithographic processes, were realized using the overlay process. The zonal placement accuracy is 1.7 nm, achieved using an internally developed alignment algorithm. Analysis of the recorded x-ray images showed that sub-15 nm resolution was achieved with the zone plates. Using this high resolution, magnetization hysteresis behaviors of magnetic structures at nanoscale have been studied. In present, we are extending the overlay fabrication process to 12 nm and even 10 nm zone plates. The preliminary result for the 12 nm zone plate shows successful fabrication of the first zone set. We expect, the 10 nm and 12 nm zone plates will yield 8 and 10 nm resolution, respectively. In this paper, a pathway to realizing multilevel zone plates by means of the overlay technique is also presented. These zone plates, when realized, can allow one to achieve sub-10 nm resolution with diffraction efficiency higher than 10%.

ACKNOWLEDGEMENTS

The authors wish to acknowledge financial support from was supported by the Division of Materials Sciences and Engineering, the Department of Energy's Office of Basic Energy Sciences.

REFERENCES

1. B. Niemann, D. Rudolph and G. Schmahl, "Soft-X-Ray Imaging Zone Plates with Large Zone Numbers for Microscopic and Spectroscopic Applications," *Opt. Commun.* **12**, 160-163 (1974).
2. G. Schmahl, D. Rudolph, B. Niemann and O. Christ, "Zone-Plate X-Ray Microscopy," *Q. Rev. Biophys.* **13**, 297-315 (1980).
3. C. Jacobsen, S. Williams, E. Anderson, M. T. Browne, C. J. Buckley, D. Kern, J. Kirz, M. Rivers and X. Zhang, "Diffraction-Limited Imaging in a Scanning-Transmission X-Ray Microscope," *Opt. Commun.* **86**, 351-364 (1991).
4. G. Schmahl and D. Rudolph Eds. *X-Ray Microscopy* (Springer-Verlag, Berlin, 1984).
5. S. Sayre, M. Howells, J. Kirz and H. Rarback Eds. *X-Ray Microscopy II* (Springer-Verlag, Berlin, 1988).
6. A. G. Michette, G. Morrison and C. J. Buckley Eds. *X-Ray Microscopy III* (Springer-Verlag, Berlin, 1992).
7. V. V. Aristov and A. I. Erko Eds. *X-Ray Microscopy IV* (Bogorodskii Press, Chernogolovka, Russia, 1994).
8. J. Thieme, G. Schmahl, D. Rudolph and E. Umbach Eds. *X-Ray Microscopy and Spectromicroscopy* (Springer-Verlag, Berlin, 1998).
9. W. Meyer-Ilse, T. Warwick and D. T. Attwood Eds. *X-Ray Microscopy VI* (American Institute of Physics, Melville, N.Y., 2000).
10. J. Susini, D. Joyeux and P. F. Eds. *X-Ray Microscopy VII* (EDP Sciences, Paris, 2003).
11. S. Aoki, Y. Kagoshima and Y. Suzuki Eds. *X-ray Microscopy VIII* (Institute of Pure and Applied Physics, Tokyo, 2006).
12. D. T. Attwood, *Soft X-Rays and Extreme Ultraviolet Radiation: Principles and Applications* (Cambridge University Press, Cambridge, U.K., 2000) 1st Edition.
13. A. G. Michette, *Optical Systems for Soft X Rays* (Plenum Press, New York, 1986).
14. W. L. Chao, E. Anderson, G. P. Denbeaux, B. Harteneck, J. A. Liddle, D. L. Olynick, A. L. Pearson, F. Salmassi, C. Y. Song and D. T. Attwood, "20-nm-Resolution Soft X-Ray Microscopy Demonstrated by Use of Multilayer Test Structures," *Opt. Lett.* **28**, 2530-2530 (2003).
15. W. Chao, E. H. Anderson, G. Denbeaux, B. Harteneck, A. L. Pearson, D. Olynick, G. Schneider and D. Attwood, "Experimental Analysis of High-Resolution Soft X-Ray Microscopy," in *X-Ray Micro- and Nano-Focusing: Applications and Techniques II*, I. McNulty Ed. Proc. SPIE **4499**, pp. 134-141 (2001).
16. K. Y. Lee, J. Frost, C. Stanley, W. Patrick, W. S. Mackie, S. P. Beaumont, and C. D. W. Wilkinson, "Fabrication of ultrasmall devices on thin active GaAs membranes," *J. Vac. Sci. Technol. B* **5**, 322-325 (1987).
17. E. H. Anderson, D. Ha and J. A. Liddle, "Sub-Pixel Alignment for Direct-Write Electron Beam Lithography," *Microelectron. Eng.* **73-74**, 74-79 (2004).
18. E. H. Anderson, V. Boegli, and L. P. Muray, "Electron Beam Lithography Digital Pattern Generator and Electronics for Generalized Curvilinear Structures," *J. Vac. Sci. Technol. B* **13**, 2529-2534 (1995).
19. W. Meyer-Ilse, H. Meddecki, L. Jochum, E. Anderson, D. Attwood, C. Magowan, R. Balhorn, M. Moronne, D. Rudolph and G. Schmahl, "New High-Resolution Zone-Plate Microscope at Beamline 6.1 of the ALS," *Synchr. Radiat. News*, **8**, (1995), pp. 29-33.
20. <http://www.cxro.lbl.gov/BL612>
21. D. Kim, P. Fischer, W. Chao, E. Anderson, S. Choe, M. Im and S. Shin, "Magnetic Soft X-Ray Microscopy at 15nm Resolution Probing Nanoscale Local Magnetic Hysteresis," *J. Appl. Phys.*, **99**, 08H303 (2006).
22. G. Schneider, "Zone plate with higher efficiency in high orders of diffraction described by dynamical theory," *Appl. Phys. Lett.* **71**, 2242 (1997).
23. S. Rehbein, G. Schneider, "Volume zone plate development at BESSY", (Institute of Pure and Applied Physics, Tokyo, 2006), pp103.